

Giant diamagnetic effect in InAs electron inversion layers measured by Zener tunneling

U. Kunze

*Institut für Technische Physik, Universität Erlangen-Nürnberg, D-8520 Erlangen, Federal Republic of Germany
and Hochmagnetfeldanlage der Technischen Universität Braunschweig, D-3300 Braunschweig, Federal Republic of Germany*

(Received 26 July 1989; revised manuscript received 20 November 1989)

Electron inversion layers on degenerate p -type InAs substrate are studied by means of Zener tunneling through the depletion layer. Two occupied subbands manifest themselves by current maxima occurring at forward biases which correspond to their minimum energies relative to the Fermi level. At magnetic fields $2.5 < B < 6.2$ T applied parallel to the surface, in the reverse-bias range the second-derivative characteristic shows new oscillations arising from diamagnetically shifted higher subbands. In contrast to the occupied subbands, the diamagnetic effect of higher subbands exceeds by a factor of 10 what is expected from the strength of the depletion field. Subband-valence-band mixing and a particular form of the surface potential well are discussed as possible reasons.

The phenomenon of a diamagnetic rise of the subband minima in quasi-two-dimensional electron systems has been widely used to study the subband structure and, in particular, to get information concerning the form of the potential well in terms of the spatial extent of the electronic wave functions. Corresponding experiments have been performed by means of optical absorption,^{1,2} transport,³⁻⁸ and tunneling.^{9,10} Among these methods, only tunneling provides a direct measure of the diamagnetic shift of higher, empty subbands.

So far, tunneling spectroscopy of the subband structure has been performed by tunneling through the oxide barrier of a metal-oxide-semiconductor (MOS) structure,^{9,10} the Schottky barrier of a metal-semiconductor contact,^{11,12} or a heterojunction semiconductor barrier.¹³⁻¹⁵ Only recently, interband tunneling between a degenerate p -type InAs electrode and an electron inversion layer has been observed in special MOS surface contacts.¹⁶ For the first time these junctions offer the possibility of studying the empty higher subbands in InAs electron inversion layers in addition to the occupied levels. We may expect the spatial extent of the excited subband's wave functions to be mainly determined by the high depletion field that is present in electron layers on degenerately doped p -type InAs, while the spread of the ground-state wave function is mainly controlled by the electric surface field as in the work of Tsui on accumulation layers on degenerate n -type InAs.⁹

The samples used in the present experiments are MOS tunnel junctions (Fig. 1) prepared on InAs(100) wafers by the same procedure as described previously.¹⁶ The bulk hole concentration at $T=77$ K amounts to 2.3×10^{17} cm⁻³, which corresponds to an energy range of empty states in the valence band of 3.3 meV at $T=0$. Metal dots of 50- μ m diameter are separated from the InAs surface by a thermally grown oxide with a thickness of a few monolayers. Because of the presence of the oxide barrier, the low work function of the Yb electrode induces a high surface-electron density as indicated in the inset of Fig. 1. The small oxide thickness also provides a low-resistive tunneling contact of the top metal to the inversion chan-

nel. Most of the applied voltage drops across the depletion layer and thus the current-voltage (I - V) characteristic is mainly determined by the Zener tunnel junction.

The I - V curve measured from a junction at $T=4.2$ K (Fig. 1) exhibits two current peaks at biases $V=42$ and 226 mV. The nearly symmetric structure of the peaks, which are imposed on a smooth background, arises from the two-dimensional character of the subbands.¹⁶ As shown recently by studies under quantizing magnetic fields,¹⁷ the current peak arising from the n th occupied

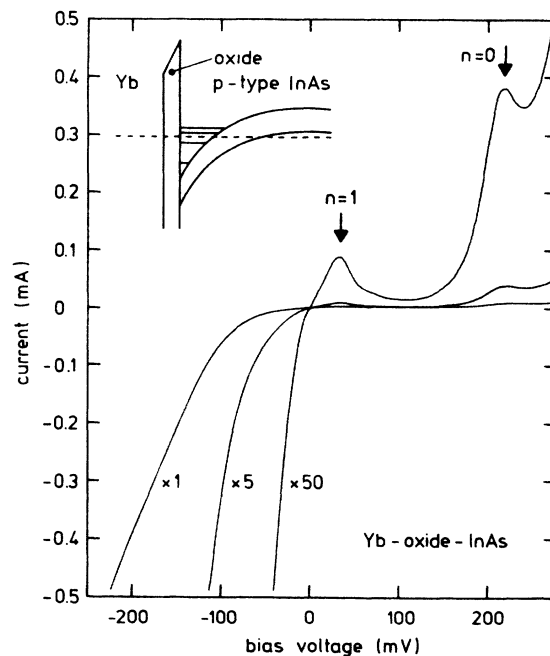


FIG. 1. Current-voltage characteristic of an Yb-oxide-InAs tunnel junction at $T=4.2$ K, whose energy-band diagram is shown in the inset (not to scale). The current peaks correspond to bottoms of occupied subbands E_n as indicated. The bias sign refers to that of the InAs electrode.

subband is centered about a bias voltage V_n where the valence-band Fermi level is aligned with the bottom E_n of the subband, $eV_n = E_F - E_n$. This is due to the fact that transverse-wave-vector conserving tunneling transitions are restricted to those states close to the subband edge where the wave vector is as small as in the empty states of the light-hole valence band. Tunneling into light-hole states is favored due to the small effective mass.

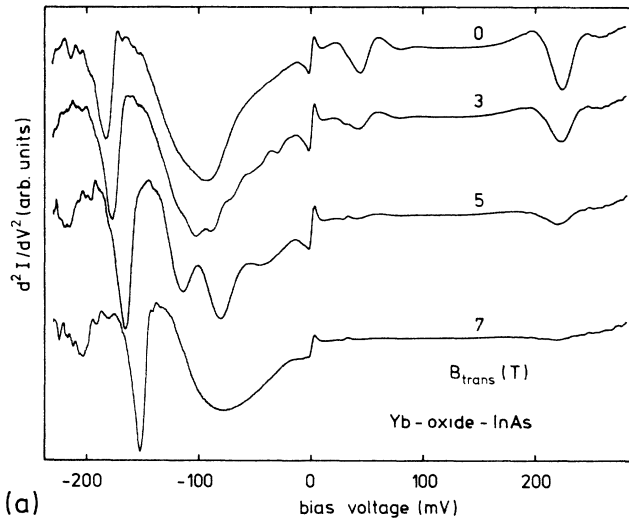
In the second derivative characteristic d^2I/dV^2 -vs- V at $B=0$ [Fig. 2(a)], the current peaks transform into M-shaped dips. Further structures, which are not of interest here, are a weak peak at $V \approx 30$ mV due to inelastic tunneling with emission of longitudinal optical phonons, a zero-bias anomaly, and a large dip at $V \approx -183$ mV, whose origin is not understood at present. When a magnetic field is applied parallel to the surface [Fig. 2(a)] new oscillations arise at reverse biases ranging from zero to $V \approx -120$ mV. Their amplitude is comparable to that of the subband-edge-induced structures. This is remarkable because in quantizing magnetic fields perpendicular to the

surface, the Landau-level structure of the occupied subbands causes oscillations in d^2I/dV^2 , whose amplitude is about 2 orders of magnitude less, except for the narrow bias ranges close to the subband-edge-induced structures where coherent tunneling occurs. Therefore in the recordings shown in Fig. 2(b), even at highest magnetic field these oscillations are not visible on the used scale. We will discuss the details of the Landau-level oscillations in a separate paper.

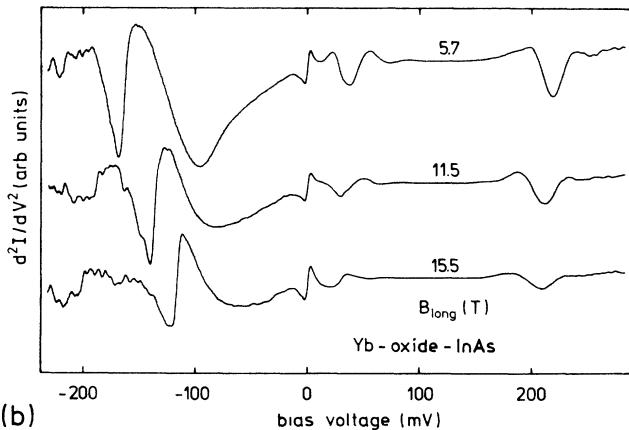
Returning to the new oscillations under parallel magnetic fields, they start rising at $B=2.5$ T and rapidly increase their amplitude and period with B . At $B=6.0$ T only one dip can be resolved, which merges at $B=6.2$ T in the broad minimum of the background curve. This should be compared with the critical magnetic field in the crossed-field configuration for vanishing electric field $F_{\text{eff}} = (F^2 - B^2 E_g / m^*)^{1/2}$ that is effective for Zener tunneling.¹⁸ Here F is the electric field in the absence of B , E_g is the energy gap, and m^* denotes the effective mass in a two-band model corresponding to the electron or light-hole effective mass. In the present sample F_{eff} decreases to zero at $B \approx 8$ T for the two occupied subbands.

A straightforward explanation of the origin of the structures can be given analogously to the tunneling spectroscopy in Si MOS junctions.¹⁰ When the Fermi level of the probing p^+ electrode is swept through the n th subband by varying the applied bias, a dip occurs in d^2I/dV^2 whose bias position V_n directly reflects the energy of the subband with respect to the Fermi level, $-eV_n = E_n - E_F$. Here the voltage drop across the oxide and the series resistance can be neglected due to the small tunneling current.

Figure 3 shows the bias positions of the dips plotted with respect to the square of magnetic field. At higher reverse biases the data points roughly follow straight lines, while at low biases, corresponding to energies close above the Fermi level, the energy variation is smaller. The latter may be due to the tailing of the higher subbands and a change of the self-consistent potential, as they become populated. The energy change of the higher subbands



(a)



(b)

FIG. 2. Second derivative d^2I/dV^2 -vs- V curve at $T=4.2$ K with different magnetic fields applied (a) transverse and (b) longitudinal with respect to the tunneling current. All curves are on the same scale. Note the new oscillations in the reverse bias range at moderate transverse magnetic fields.

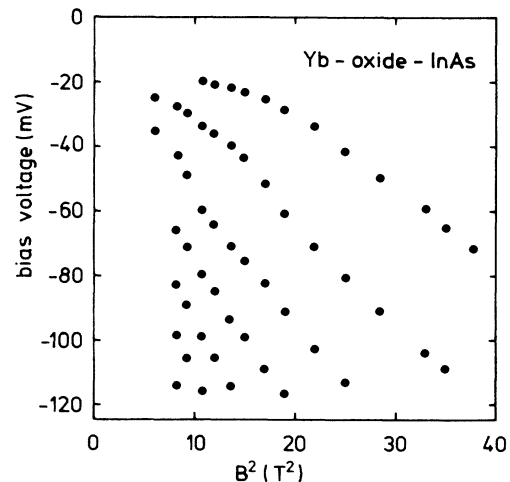


FIG. 3. Bias positions of the minima of the new oscillations in d^2I/dV^2 as shown in Fig. 2, as a function of the square of the magnetic field.

should be compared with the small shifts of the $n=0$ and $n=1$ subbands. At $B=5$ T the Fermi energy $E_F - E_0$ is reduced by about 4 meV from its zero-field value, while the separation $E_1 - E_0$ even remains unchanged within experimental accuracy of ± 2 meV. These small changes, which contain both the diamagnetic shift and a density-of-states increase,¹⁰ justify an evaluation of the shift of the higher subbands in terms of a diamagnetic effect. The diamagnetic shift $\Delta E_n = -e\Delta V_n$ is given by $\Delta E_n = -e^2 B^2 \delta_n^2 / 2m^*$, where $\delta_n = (\langle z^2 \rangle - \langle z \rangle^2)^{1/2}$ represents the spread of the wave function perpendicular to the interface. The slopes of straight lines fitted to the data points yield estimates for the spread δ_n ranging from 25 to 44 nm for $n=2$ (top curve) to $n=7$, respectively. Another item worth mentioning is the small energy separations of the $n \geq 2$ subbands of 5–10 meV at $B=0$, as gained from extrapolations of the data points in Fig. 3.

The energy separations in the present sample should be compared with recent self-consistent calculations of the subband structure in InAs n -inversion layers.¹⁹ Although the calculation is based on a smaller bulk acceptor concentration (10^{17} cm^{-3}) than that of the present samples ($2.3 \times 10^{17} \text{ cm}^{-3}$), the resulting energy separation $E_2 - E_1 \approx 100$ meV is larger than the measured value of about 60 meV. The spread of the wave function can be estimated from the simple triangular-well model,²⁰ where only the depletion field at the InAs surface of $F_{\text{depl}} \approx 2 \times 10^7 \text{ V/m}$ has been taken into account. The resulting spread is smaller than the experimental results by more than a factor of 3, corresponding to a difference in the diamagnetic effect of a factor of 10. It should be clear that this large discrepancy can hardly be attributed to the incorrect triangular potential which neglects the finite depletion-layer width of about 70 nm. Also, the change of

the depletion field due to the change of the tunneling voltage should only cause small energy shifts. A possible explanation is subband–valence-band mixing,²¹ which leads to a rise of the energies in particular of the lower subbands, thus decreasing the subband separations. However, due to the large energy gap of InAs, we may suspect the Zener tunneling to have minor influence on the subband structure. Another possible mechanism leading to small energy separations between excited subbands and to large extension of the wave functions is a wide surface potential well. If a compensating donor layer is present due to stoichiometric defects that may be generated during the growth of the oxide layer, the depletion field close to the surface vanishes, while the interband tunnel junction is shifted deeper into the bulk. So far we have explained the observed energy shifts in terms of a diamagnetic effect that is detected by tunneling spectroscopy from the valence-band Fermi level. This picture need not be correct; e.g., it seems unclear whether the lateral displacement of the $E(k)$ subband parabolas in a parallel magnetic field influences the bias threshold for the onset of Zener tunneling.

In conclusion, we have demonstrated the use of Zener tunneling for tunneling spectroscopy of the subband structure in InAs electron inversion layers. In magnetic fields parallel to the surface, the diamagnetic rise of higher empty subbands, as determined from a bias shift of corresponding structures in d^2I/dV^2 , is much larger than expected from simple estimates. However, a self-consistent calculation of the subband structure and of the Zener tunneling current under parallel magnetic field, including subband–valence-band mixing, seems desirable so as to obtain a conclusive interpretation of the experimental facts.

¹W. Beinvoogl, A. Kamgar, and J. F. Koch, Phys. Rev. B **14**, 4274 (1976).

²U. Merkt, Phys. Rev. B **32**, 6699 (1985).

³R. E. Doezema, M. Nealon, and S. Whitmore, Phys. Rev. Lett. **45**, 1593 (1980).

⁴Th. Englert, J. C. Maan, D. C. Tsui, and A. C. Gossard, Solid State Commun. **45**, 989 (1983).

⁵J. Yoshino, H. Sakaki, and T. Hotta, Surf. Sci. **142**, 326 (1984).

⁶W. Zhao, F. Koch, J. Ziegler, and H. Maier, Phys. Rev. B **31**, 2416 (1985).

⁷A. Zrenner, H. Reisinger, F. Koch, K. Ploog, and J. C. Maan, Phys. Rev. B **33**, 5607 (1986).

⁸W. Cheng, A. Zrenner, Q. Ye, F. Koch, D. Grützmacher, and P. Balk, Semicond. Sci. Technol. **4**, 16 (1989).

⁹D. C. Tsui, Solid State Commun. **9**, 1789 (1971).

¹⁰U. Kunze, Surf. Sci. **170**, 353 (1986); Solid State Commun. **61**, 543 (1987); Phys. Rev. B **35**, 9168 (1987); Surf. Sci. **196**, 374 (1988).

¹¹M. Zachau, F. Koch, K. Ploog, P. Roentgen, and H. Beneking, Solid State Commun. **59**, 591 (1986).

¹²H. P. Zeindl, T. Weghaupt, I. Eisele, H. Oppolzer, H. Reisinger, G. Tempel, and F. Koch, Appl. Phys. Lett. **50**, 1164 (1987).

¹³T. W. Hickmott, Phys. Rev. B **32**, 6531 (1985); Solid State Commun. **63**, 371 (1987).

¹⁴J. Smoliner, E. Gornik, and G. Weimann, Solid State Commun. **52**, 2136 (1988).

¹⁵For an example of recent work on multisubband resonant tunneling see, e.g., S. Sen, F. Capasso, A. C. Gossard, R. A. Spah, A. L. Hutchinson, and S. N. G. Chu, Appl. Phys. Lett. **51**, 1428 (1987).

¹⁶U. Kunze and W. Kowalsky, Appl. Phys. Lett. **53**, 367 (1988).

¹⁷U. Kunze, Appl. Phys. Lett. **54**, 2213 (1989).

¹⁸M. H. Weiler, W. Zawadzki, and B. Lax, Phys. Rev. **163**, 733 (1967).

¹⁹H. Übensee, G. Paasch, and G. Gobsch, Solid State Commun. **62**, 699 (1987).

²⁰F. Stern, Phys. Rev. B **5**, 4891 (1972).

²¹A. Ziegler and U. Rössler, Solid State Commun. **65**, 805 (1988).